Studies on MCM–D interconnections

Speaker: *Peter Gerlach*
Department of Physics
Bergische Universität Wuppertal
D-42097 Wuppertal, GERMANY

Authors:
K.H.Becks, T.Flick, P.Gerlach, C.Grah, P.Mättig
Department of Physics
Bergische Universität Wuppertal
D-42097 Wuppertal, GERMANY
T.Rohe[1]
Max-Planck-Institut für Physik
Föhringer Ring 6
D-80805 München, GERMANY
for the ATLAS Pixel Collaboration

1 Abstract

In the context of the development of the ATLAS Pixel Detector [1], a multi chip module technology called MCM–D (multi chip module deposited) has been studied to implement the high density interconnect. The results of some first assemblies using 'standard' sensor designs have been reported in [2].

The focus of this note is on the first results of assemblies optimized to the capabilities of this technology, namely the possibility to build uniformly segmented sensors. Special attention is spent to the studied option of an 'equal sized bricked' sensor design.

2 Introduction

Multi Chip Module Deposited uses BCB (Benzo Cyclo Butene, CYCLOTENE^{TM}, Dow Chemical Inc., USA) and copper to deposit connecting structures. This is done by

[1]Present address: Paul Scherrer Institut, CH-5232 Villigen PSI, SWITZERLAND

using wafer level techniques as spin-on, sputtering, and electro–plating. Five layers of dielectric/conductor film–pairs are deposited in this way, forming both the power supply lines and the signal connections as well as the passivation and pad metallization layer.

The idea is to place all connections needed between the integrated circuits on the sensor. This takes advantage of the hybrid pixel device approach and allows to use bump bonding as the only assembly technique.

Since all the intra-connection structures are placed on the sensor, the choice of materials used and their process parameters (e.g. temperatures) are a critical issue. For this reason, and because of it's low specific dielectric constant of $\epsilon_r = 2.7$ (1 MHz), BCB has been chosen as dielectric material.

The thickness of the copper layers is determined by the voltage drop on the power supply lines, so that at maximal voltage difference one can still operate all electronic chips properly. To minimize this voltage drop within the parameters of the process, four metal layers are build of 3.5 µm thick copper each. The signal lines are placed above a ground plane to build a micro strip line configuration. This ensures high signal quality and low crosstalk between neighbouring lines.

The assembly and test of a fully featured prototype module has been reported before [2]. The following is dedicated to the fact that integrating the module intra-connection structures on the sensor provides an additional freedom:
There are small structures (called 'feed-throughs') connecting every sensor cell with it's corresponding electronic circuit. These feed-throughs allow an adaption between different segmentations of the sensor and the electronic chip used to build the hybrid. Particularly with regard to the gap between two chips on a module this brings a favourable solution of avoiding inactive areas. Because of an inactive area at the chip edges of about 100 µm and an additional space between two chips of another 200 µm one has to deal with a gap of 400 µm. Instead of using ganged or enlarged sensor cells, done in the standard design, with MCM–D it is possible to use equal-sized sensor cells and perform the routing between the contact pads in the MCM–D layers.

Building up single chip devices gives the possibility to prove the technology and measure the electrical characteristics of such an equal-sized bricked sensor with routing in MCM–D-structures.

3 Tests with 'Standard' Parts

To test the routing capability of the feed-throughs, a design had been implemented as shown in fig. 1. The bump pads of the sensor are used as contact area for the first copper layer. These bump pads are fitting the geometry of the ones on the electronic chips; they also have to be able to be hybridized without thin film layers. To 'simulate' a different segmentation of the two parts, not all feed-throughs are connecting the

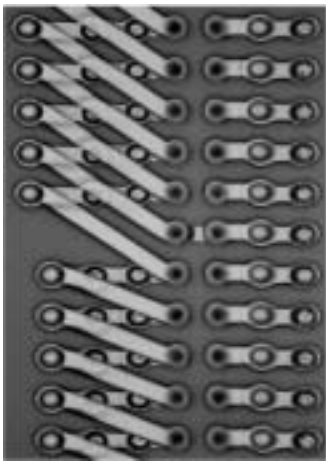

Figure 1: First test structure with routed pixel cells

cells one to one (fig. 1: standard feed-through, right column). Some feed-throughs are connecting the sensor cell to it's neighbouring electronic cell, some are skipping more than one electronic cell (fig. 1: left column).

It has been shown in [2] that the influence of the routing on the performance of the electronic chip is negligible, as long as crossing of copper lines in adjacent metal layers can be avoided.

4 Optimized Devices

A set of single chip assemblies has been produced using the ATLAS front end chip (18×160 cells of $50\,\mu\text{m} \times 400\,\mu\text{m}$ with a mirrored bump pad geometry) and sensors especially designed for this purpose. These hybrids feature equal-sized and equal-sized-bricked sensor geometries and complex routing schemes in MCM–D technology.

4.1 Sensor Design

Three different types of p-spray isolated 'n^+-on-n' single chip sensors were used. They were placed on the same wafers as used for baseline ATLAS pixel sensors and therefore share the technology described in [3, 4, 5].

The design is also done according to the base line production sensors in respect of the gap size between pixel implants and the implementation of the bias grid (bias dot).

A single chip sensor covers the area of one readout chip. In order to simulate the 'dead' chip region occuring in a 16-chip module, as mentioned before, the sensor's

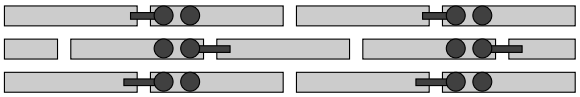

Figure 2: Bricked pixel pattern with a mirrored bump pad geometry.

sensitive area is extended by 200 µm in both direction. In all three sensors this additional area is covered by distributing it equally on all pixels. This results in a uniform pixel pitch of 51.25 µm × 422.22 µm that differs from the pitch of the electronics. MCM–D is used to route the signals to the pads of the preamplifiers. In one of the three devices tested this is the only difference to the standard sensors which were used as reference.

Two further sensors feature a bricked pixel geometry meaning that the pixels of adjacent rows are shifted by 1/4 of the pitch in altering directions as shown in fig. 2. This improves the spatial resolution along the z-axis by a factor of two, in case of double hits. However the bricked geometry is not compatible with the mirrored bump pad pattern as the pad of every second pixel has to be placed on top of its neighbour (fig. 2). If this routing is done in the sensor's metallization this will lead to large additional capacitances as the covering oxide is very thin (about 200 nm) and therefore this option is only seriously considered in combination with MCM–D. In the devices discussed here, in addition the different pitch of readout chip and sensor requires additional routing anyway. In order to obtain a rectangular shape of the sensitive area, the pixels of the two outer columns were cut to 3/4 resp. extended to 5/4 of the pixel length.

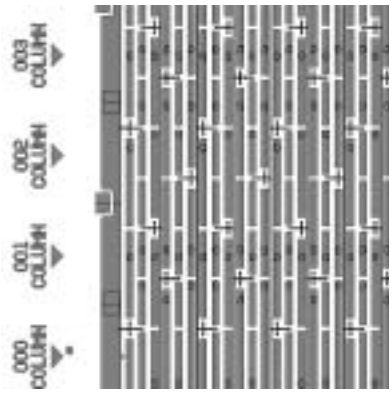

Figure 3: Biasgrid in parallel geometry.

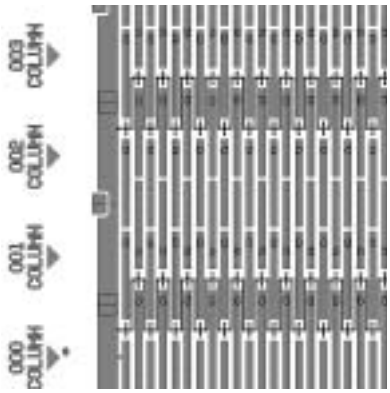

Figure 4: Biasgrid in 'zigg-zagg' pattern.

The implementation of a bias grid in a bricked pixel geometry is problematic as metal bus lines cannot run straight and parallel to the short pixel sides. Two

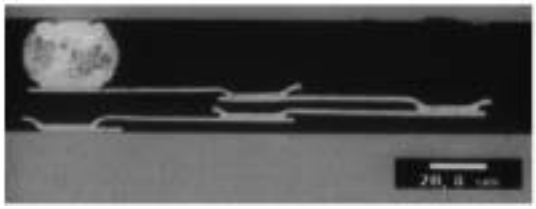

Figure 5: Cross section of a feed-through structure.

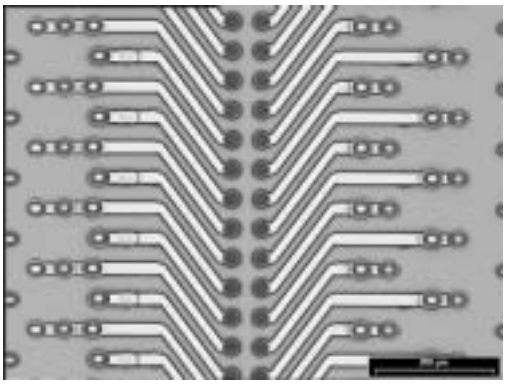

Figure 6: Routing on an equal-sized-bricked sensor.

implementations were tested. One following the pixel borders in a 'zigg-zagg' pattern, the other is following the long pixel edge in every 3rd row biasing two rows at either side with tree like branches. Fig. 4 and fig. 3 show the design implementation for the topmost metal layer of the sensor.

4.2 Feed–Through Structures

A 'standard' sensor implements the smallest possible feed-through structure. This is shown in a cross section figure 5. It uses copper lines with a width 20 µm and a via–pitch of 50 µm.

The same linewidth was used in the equal-sized design. Here the sensor and electronic cells are placed above each other at one end of the columns (near the 'end of column logic'). Due to the difference between the short dimension of two cells (50 µm and 51.25 µm), the distance to be covered increases with the row number up to 200 µm. The mismatch between the long dimension leads to *no* differences here as the contact placements on the sensor (to the first copper layer) has been optimized.

To allow for a gap between opposing front end chips on a module, the 'outer' rows of sensor and electronic cells have to be placed on top of each other. For the 'equal sized bricked' sensor geometry, this means that even with an electronic chip centred along the long direction of the cells with respect to the sensor area, the routing has to be quite dense, as shown in figure 6. To avoid any crossings of copper lines, the width of the traces are reduced to 15 µm, with a minimal gap of 15 µm. Based on the small number of devices built up to now, no loss in the connection yield of the feed-throughs could be monitored. Special designed devices with daisy chained feed-throughs will be investigated in the near future to prove the reliability of the connections.

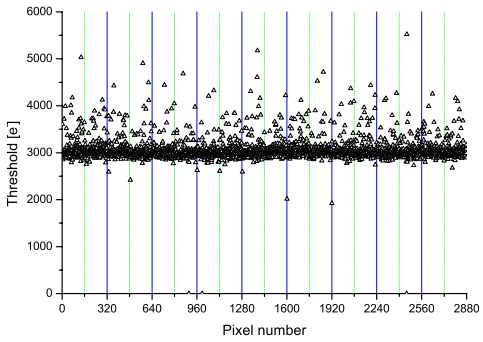

Figure 7: Threshold distribution of equal-sized-bricked hybrid.

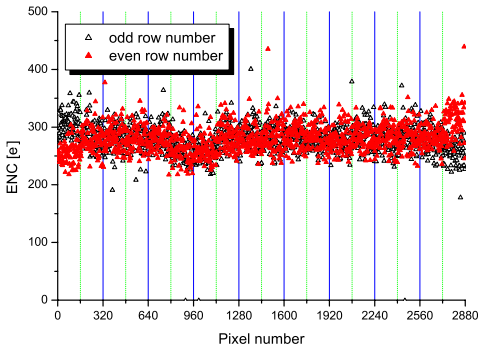

Figure 8: Equivalent noise charge of equal-sized-bricked hybrid, uncovering the shorter cells in first and last column.

5 Electrical Tests on Equal-sized-bricked Devices

The ATLAS Pixel front end chip implements a threshold, tunable individually for each pixel cell. The amount of charge collected by the cell is measured as the time over threshold (TOT) of the output of the current feedback amplifier. This time is measured as number of clock cycles [6, 7].

Measuring the tuned thresholds of an equal-sized-bricked hybrid, one observes a uniform distribution as illustrated in figure 7. The equivalent noise charge (fig. 8) uncovers the 3/4 and 5/4 long sensor cells in the first and last column. The routing implementation without crossing feed-throughs leaves the sensor cell size as the dominant factor on the performance.

6 First Results on Test Beam Measurements

In August 2002, with great support from the ATLAS Pixel community, an extensive test beam program has been performed with these single chip hybrids. Several million events, taken at different angles in θ and ϕ (so, rotations around the long and the short axis of the cells), have been recorded. Fig. 9 shows a beam profile, taken with an equal sized bricked device at 0°.

Investigating the location of a hit, predicted by the beam telescope, the $\pm 1/4$ shifted cells are clearly visible, as shown in fig. 10. The charge collected in single and multiple hits is illustrated in fig. 11. A fit of a Landau distribution is not adaptable as the calibration of the TOT values is not yet done.

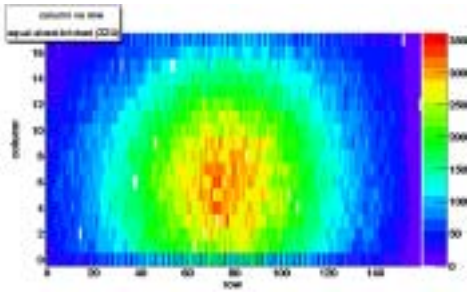

Figure 9: Hitmap of an equal-sized-bricked hybrid showing the beam profile (13 pixel cells masked to read out).

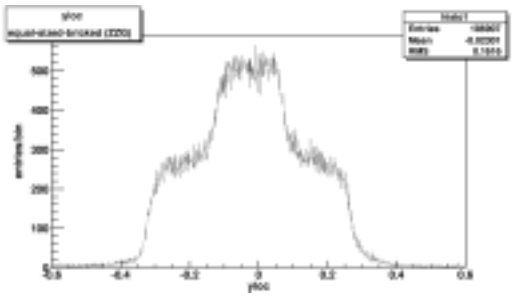

Figure 10: Difference between measured and estimated y-location. Shift of 1/2 cell-size clearly visible.

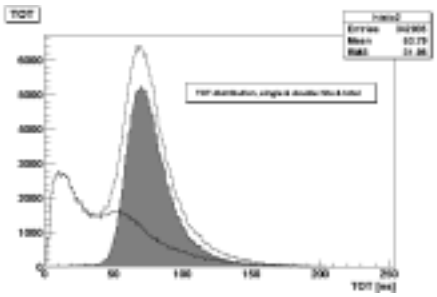

Figure 11: Charge collection of the chip, single hits (grey) and double hits are distinguished.

7 Conclusions

Equal sized bricked pixel detector devices has been implemented, making use one of the benefits of the MCM–D technology. The first results of electrical and test beam measurements are showing an excellent, uniform behaviour. The size of the sensor cells is dominating the performance of the individual pixels.

Further measurements on these devices and the analysis of data taken will investigate the crosstalk and the spatial resolution for multiple hits.

Acknowledgement

The authors wish to thank the test beam crew of the ATLAS Pixel collaboration for their support and the Fraunhofer Institute IZM, Berlin, especially their MCM–D project coordinator K. Scherpinski and the clean-room staff, for their great effort.

References

[1] M. S. Alam *et al.* [ATLAS Collaboration], "ATLAS pixel detector:Technical design report," CERN-LHCC-98-13.

[2] C. Grah [ATLAS Pixel Collaboration], "Pixel Detector Modules Using MCM–D Technology," Nucl. Instrum. Meth. A **465**, 211 (2000).

[3] M. S. Alam *et al.*, "The ATLAS silicon pixel sensors," Nucl. Instrum. Meth. A **456**, 217 (2001).

[4] T. Rohe [ATLAS Pixel Collaboration], "Design And Test Of Pixel Sensors For The Atlas Pixel Detector," Nucl. Instrum. Meth. A **460**, 55 (2001).

[5] R. Wunstorf, "Radiation Tolerant Sensors For The Atlas Pixel Detector," Nucl. Instrum. Meth. A **466**, 327 (2001).

[6] J. Richardson [ATLAS Pixel Collaboration], "Performance Measurements of ATLAS Pixel Electronics," PIXEL2002 International Workshop on Semiconductor Pixel Detectors for Particles and X-Rays, Carmel California, September 2002.

[7] J. Richardson [ATLAS Pixel Collaboration], "The ATLAS Pixel On-Detector Electronics," 5th Workshop of LHC Electronics, Snowmass Colorado, September 1999.